Dyes and Pigments 94 (2012) 583–591

Contents lists available at SciVerse ScienceDirect

Dyes and Pigments

journal homepage: www.elsevier.com/locate/dyepig

Synthesis and optical properties of 6,10-dihydrofluoreno[2,3-*d*:6,7-*d*′]diimidazole derivatives

Hong-Fang Chen, Yong-Mei Cui*, Jian-Guang Guo, Hai-Xia Lin**

Department of Chemistry, College of Sciences, Shanghai University, 99 Shangda Road, Baoshan District, Shanghai 200444, PR China

A R T I C L E I N F O

Article history:
Received 5 January 2012
Received in revised form
22 February 2012
Accepted 5 March 2012
Available online 21 March 2012

Keywords:
Synthesis
Fluorene
Imidazole
Synthesis
UV absorption
Fluorescence

A B S T R A C T

A series of 10,10-dioctyl-3,6-dihydrofluoreno[2,3-*d*:6,7-*d*′]diimidazole derivatives were conveniently synthesized by condensation of the key intermediate 2,3,6,7-tetraamino-9,9-dioctylfluorene (TADOF) with aldehydes under very mild conditions. All of the target compounds were characterized using ^{1}H NMR, ^{13}C NMR, and elemental analysis. The crystal structure of 3,6-dibenzyl-10,10-dioctyl-2,7-diphenyl-6,10-dihydro-3H-fluoreno[2,3-*d*:6,7-*d*′]diimidazole was determined as triclinic, space group P-1 type, using single X-ray crystallography. For seventeen samples, UV–visible absorption maximum wavelength (λ_{max}), fluorescence excitation wavelength (λ_{ex}), fluorescence emission wavelength (λ_{em}) and fluorescence quantum yield (φ_{FL}) were measured in dilute dichloromethane solution and in the solid state. These compounds possess a medium strong blue fluorescence-emitting ability with φ_{FL} values in the region of 0.30–0.89 and structure-optical behavior characteristics were discussed.

1. Introduction

Since the reports by C. W. Tang [1] and J. H. Burroughes [2], organic and polymer light-emitting diode (LED) materials have received considerable attention due to their potential application in various displays [3–8], and enormous efforts have been made toward the development of new high-performance materials with desirable properties [9–23]. Due to their rigid planarized oligophenyl unit within the backbone as well as the possibility of facile functionalization at the methylene bridge, fluorene-based derivatives, including polymers and oligomers, exhibit unique photoluminescent properties and have been widely used as lumin escent materials [24–28], as well as carrier transport materials for filed effect transistors (FETs) [29–31]. However, small-molecule fluorene derivatives with good thermal stability and high photoluminescence (PL) efficiency have been little reported [32–35]. Fluorescent heterocyclic compounds are of interest in many areas such as emitters for electroluminescence devices, molecular probes for biochemical research, in traditional textile and polymer fields, fluorescent whitening agents and photoconducting materials [36–38]. Imidazole derivatives are important five-membered nitrogen-containing electron-accepting heterocyclic compounds with broad spectrum of biological activities and have potential applications in electrical and optical materials. Fluorescent characteristics rely largely on molecular structure and molecular assembly. Changes in the substitutional groups and substitution pattern, conjugation, and molecular electronic structure can bring about very different optical and physical properties for such materials. There is presently great interest to increase the structural or spatial dimensions of π-conjugated molecules in order to tune and acquire more favorable physical properties.

We recently presented detailed structure–property relationship investigations into new fluorene derivatives based on 3,9-dihydro-9,9-dioctylfluoreno[3,2-*d*]imidazole (DOFI) and found that their electronic absorption and emission profiles exhibited sensitivity to functional group substitution pattern [39]. As an expanded continuation of our studies related to the synthesis and optical properties of heterocycle-based chromophores, in this paper, we present the initial synthesis and characterization of a series of novel 6,10-dihydrofluoreno[2,3-*d*:6,7-*d*′]diimidazole derivatives. It is envisioned that the fusion of another aryl-imidazole unit into the skeleton can improve their photo-electric properties. Similarly, two octyl groups were introduced to the C-9 position of the fluorene

---

* Corresponding author. Tel.: +86 21 66132190; fax: +86 21 66134594.
** Corresponding author. Tel.: +86 21 66136050; fax: +86 21 66133039.
E-mail addresses: ymcui80@gmail.com, ymcui@shu.edu.cn (Y.-M. Cui), haixialin@staff.shu.edu.cn (H.-X. Lin).

0143-7208/$ – see front matter © 2012 Elsevier Ltd. All rights reserved.
doi:10.1016/j.dyepig.2012.03.004

moiety to increase solubility as well as to release intermolecular π-π stacking. And we focused our attention on 10,10-dioctyl-3,6-dihydrofluoreno[2,3-*d*:6,7-*d*′]diimidazoles (DOFDIs) with different terminal aryl ring to investigate their UV–visible absorption and fluorescence characters. The synthetic pathway and the structures of the target molecules are shown in Figs. 1 and 2.

2. Experimental

2.1. Reagents and instruments

Commercially available reagents were purchased and were used without further purification unless otherwise mentioned. ^{1}H NMR and ^{13}C NMR spectra were recorded on a Bruker Avance (500 MHz) spectrometer in $CDCl_3$ or DMSO-d_6, unless otherwise noted. Chemical shifts are reported in parts per million (ppm) and coupling constants (*J*) are reported in Hertz (Hz). Coupling patterns are described by abbreviations: s (singlet), d (doublet), t (triplet), m (multiplet), br (broad). Chemical shifts were reported in the scale relative to $CHCl_3$ (7.26 ppm) or DMSO-d_6 (2.50 ppm) for ^{1}H NMR, and to $CDCl_3$ (77.16 ppm) or DMSO-d_6 (39.70 ppm) for ^{13}C NMR, as internal references. The center line of the multiplets of DMSO-d_6 was defined as 2.50 for ^{1}H NMR. Silica gel plate GF254 was used for thin layer chromatography (TLC) and silica gel 300–400 mesh was used for flash column chromatography. Melting points were measured on a Digital Melting Point Apparatus without correction. Yields are shown in terms of those isolated pure materials. The absorption and fluorescence spectra were recorded using a UV-2501Pc spectrophotometer and an RF-5301 fluorescence spectrophotometer. Elemental analysis was performed on an Elementary Vario EL (Germany) instrument. MS were taken with an Agilent LCMS-1100.

2.2. Synthesis

2.2.1. General procedure for the synthesis of 3a-o

To a suspension of 3,6-dinitro-9,9-dioctylfluorene-2,7-diamine [40] (230 mg, 0.45 mmol) in ethanol (30 mL) was added $Pd(OH)_2$ (50 mg, 0.16 mmol). The reaction mixture was heated to 90 °C with stirring, and then hydrazine hydrate (1.32 g, 26.4 mmol) was added dropwise. The reaction mixture was stirred at 90 °C for 20 min, and then cooled, filtered and the mixture was extracted with AcOEt for three times. The combined organic layer was washed with brine, dried over Na_2SO_4, filtered, and then the solvent was evaporated in vacuum. The obtained yellow residue 2,3,6,7-tetraamino-9,9-dioctylfluorene **2a** was directly used for next step without further purification.

A mixture of the corresponding aldehyde (0.889 mmol) and **2a** obtained above in 1,4-dioxane was refluxed for about 10 h. The solvent was removed under vacuum and the residue was purified by flash column chromatography using petroleum ether/ethyl acetate as eluent to afford the desired compounds **3a-o** in 20–75% yields for two steps.

*2.2.1.1. 10,10-Dioctyl-2,7-diphenyl-6,10-dihydro-3H-fluoreno[2,3-d:6,7-d′]diimidazole (**3a**).* White powder, yield 60%. Mp 189–190 °C ^{1}H NMR (500 MHz, DMSO-d_6): δ ppm 0.55 (m, 4H), 0.71 (t, *J* = 7.1 Hz, 6H), 0.97–1.07 (m, 20H), 2.06 (m, 4H), 7.45 (m, 1H), 7.48–7.51 (m, 2H), 7.55–7.58 (m, 4H), 7.62 (m, 1H), 7.89 (d, *J* = 11.1 Hz, 1H), 8.11–8.15 (m, 1H), 8.17–8.20 (m, 4H), 12.81–12.92 (m, 2H). ^{13}C NMR (125 MHz, DMSO-d_6): δ ppm 13.9, 22.1, 23.7, 28.7, 28.9, 29.5, 31.2, 41.4, 53.5, 101.4, 101.6, 105.2, 109.3, 112.8, 126.3, 129.0, 129.6, 130.6, 134.9, 136.2, 136.9, 137.1, 143.9, 144.8, 145.3, 145.9, 146.4, 151.2. Anal. calculated for $C_{43}H_{50}N_4$: C, 82.91; H, 8.09; N, 8.99. Found: C, 82.78; H, 7.96; N, 9.16.

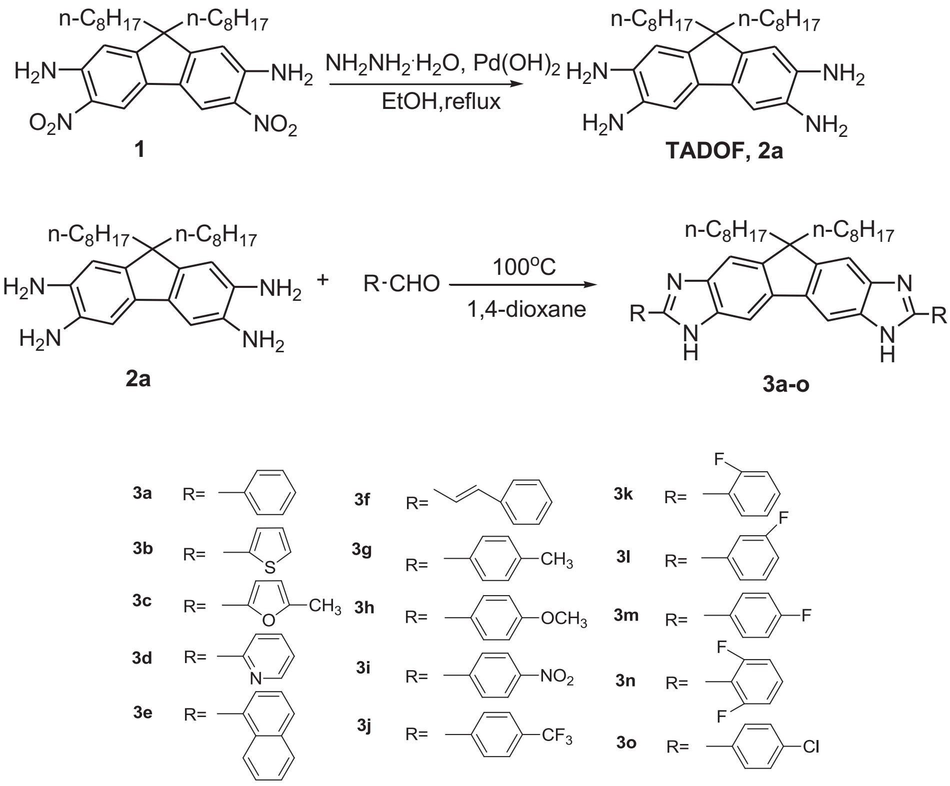

Fig. 1. The synthetic route of the 6,10-dihydrofluoreno[2,3-*d*:6,7-*d*′]diimidazole derivatives **3a-o**.

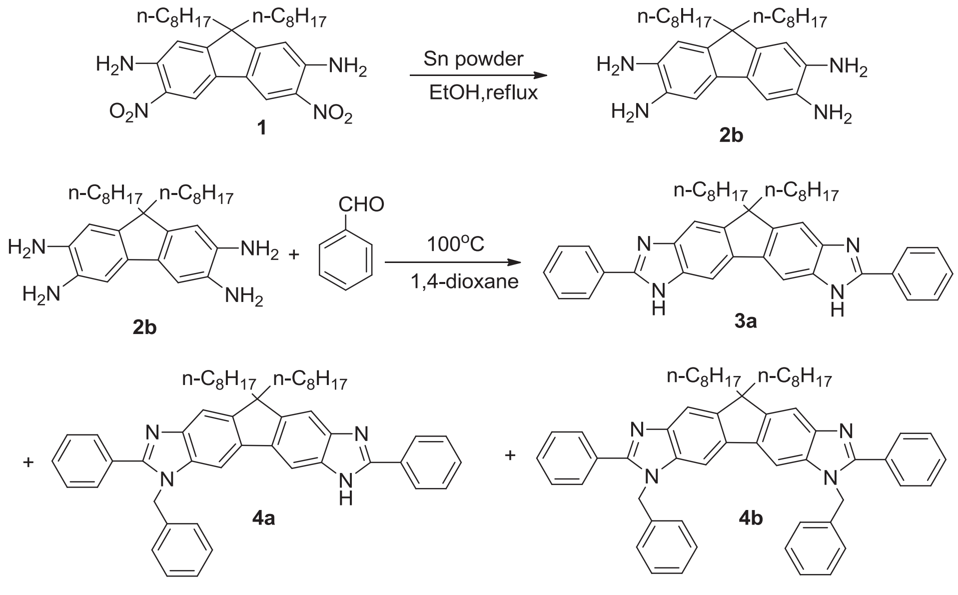

Fig. 2. The synthesis of compounds **4a-b**.

*2.2.1.2. 10,10-Dioctyl-2,7-di(thiophen-2-yl)-6,10-dihydro-3H-fluoreno[2,3-d:6,7-d′]diimidazole (**3b**).* Light yellow powder, yield 40%. Mp 145–147 °C ^{1}H NMR (500 MHz, DMSO-d_6): δ ppm 0.51 (m, 4H), 0.70 (t, J = 7.2 Hz, 6H), 0.94–1.00 (m, 20H), 2.01 (m, 4H), 7.23 (m, 2H), 7.41 (s, 1H), 7.55 (s, 1H), 7.69–7.71 (m, 2H), 7.81–7.84 (m, 2H), 7.87 (s, 1H), 8.07 (m, 1H), 12.85–12.94 (m, 2H). ^{13}C NMR (125 MHz, DMSO-d_6): δ ppm 13.9, 14.0, 20.1, 22.1, 22.2, 23.7, 28.7, 28.8, 29.1, 29.4, 29.5, 31.2, 31.4, 31.6, 41.2, 41.3, 53.7, 101.2, 101.5, 105.0, 109.0, 112.5, 126.3, 128.3, 128.5, 134.2, 134.6, 134.8, 136.2, 137.0, 137.1, 143.6, 143.9, 144.9, 145.4, 146.0, 146.5, 147.0, 147.1. Anal. calculated for $C_{39}H_{46}N_4S_2$ C, 73.77; H, 7.30; N, 8.82. Found: C, 73.74; H, 7.27; N, 8.90.

*2.2.1.3. 2,7-Bis(5-methylfuran-2-yl)-10,10-dioctyl-6,10-dihydro-3H-fluoreno[2,3-d:6,7-d′]diimidazole (**3c**).* Yellow powder, yield 36%. Mp 181–183 °C ^{1}H NMR (500 MHz, DMSO-d_6): δ ppm 0.51 (m, 4H), 0.71 (t, J = 7.1 Hz, 6H), 0.92–1.03 (m, 20H), 1.99–2.01 (m, 4H), 2.42 (s, 6H), 6.34 (m, 2H), 7.06 (m, 2H), 7.39 (s, 1H), 7.52 (s, 1H), 7.80 (s, 1H), 8.00 (s, 1H), 12.74–12.79 (m, 2H). ^{13}C NMR (125 MHz, DMSO-d_6): δ ppm 13.6, 13.9, 22.1, 23.7, 28.7, 28.9, 29.2, 29.5, 31.2, 41.3, 53.4, 101.3, 105.1, 108.6, 111.1, 112.4, 134.1, 136.2, 136.7, 143.8, 144.4, 153.5. Anal. calculated for $C_{41}H_{50}N_4O_2$ C, 78.06; H, 7.99; N, 8.88. Found: C, 78.18; H, 8.02; N, 8.68.

*2.2.1.4. 10,10-Dioctyl-2,7-di(pyridin-2-yl)-6,10-dihydro-3H-fluoreno[2,3-d:6,7-d′]diimidazole (**3d**).* Light yellow powder, yield 46%. Mp 114–115 °C ^{1}H NMR (500 MHz, DMSO-d_6): δ ppm 0.48 (m, 4H), 0.62 (m, J = 7.1 Hz, 6H), 0.87–0.98 (m, 20H), 1.91–1.96 (m, 4H), 7.45 (m, 3H), 7.65 (s, 1H), 7.83–7.90 (m, 1H), 7.95 (m, 2H), 8.10–8.18 (m, 1H), 8.34 (m, 2H), 8.70 (m, 2H), 13.12 (m, 2H). ^{13}C NMR (125 MHz, DMSO-d_6): δ ppm 13.9, 22.0, 23.7, 28.7, 28.9, 29.5, 31.2, 41.5, 53.5, 102.0, 105.8, 109.5, 113.2, 121.3, 124.4, 134.9, 136.4, 137.5, 144.0, 144.3, 145.1, 145.6, 146.5, 147.1, 148.8, 149.4, 150.8. Anal. calculated for $C_{41}H_{48}N_6$ C, 78.81; H, 7.74; N, 13.45. Found: C, 78.95; H, 7.82; N, 13.64.

*2.2.1.5. 2,7-Di(naphthalen-1-yl)-10,10-dioctyl-6,10-dihydro-3H-fluoreno[2,3-d:6,7-d′]diimidazole (**3e**).* Light yellow powder, yield 44%. Mp 180–192 °C ^{1}H NMR (500 MHz, DMSO-d_6): δ ppm 0.55 (s, 4H), 0.65 (t, J = 7.0 Hz, 6H), 0.93–1.02 (m, 20H), 2.00 (m, 4H), 7.47 (s, 1H), 7.58–7.59 (m, 2H), 7.63 (m, 2H), 7.66–7.71 (m, 3H), 7.96 (m, 1H), 8.01 (d, J = 7.6 Hz, 2H), 8.05–8.07 (m, J = 7.9 Hz, 4H), 8.26 (s, 1H), 9.28 (m, 2H), 12.97–13.02 (m, 2H). ^{13}C NMR (125 MHz, DMSO-d_6): δ ppm 13.9, 22.1, 23.7, 28.7, 28.9, 29.1, 29.6, 31.2, 41.5, 53.6, 101.6, 105.2, 109.5, 112.9, 125.4, 126.4, 126.7, 127.0, 127.7, 128.5, 130.0, 130.7, 133.8, 134.4, 136.3, 137.1, 144.0, 144.8, 145.4, 146.0, 146.6, 151.4. Anal. calculated for $C_{51}H_{54}N_4$: C, 84.72; H, 7.53; N, 7.75. Found: C, 84.52; H, 7.68; N, 7.64.

*2.2.1.6. 10,10-Dioctyl-2,7-di((E)-styryl)-6,10-dihydro-3H-fluoreno[2,3-d:6,7-d′]diimidazole (**3f**).* Yellow powder, yield 38%. Mp 176–178 °C ^{1}H NMR (500 MHz, DMSO-d_6): δ ppm 0.51 (m, 4H), 0.69 (t, J = 7.0 Hz, 6H), 0.93–0.98 (m, 20H), 1.97 (m, 4H), 7.21–7.24 (m, 1H), 7.28 (s, 1H), 7.33 (m, 2H), 7.41 (m, 4H), 7.50 (m, 2H), 7.65–7.68 (m, 5H), 7.95 (s, 2H), 12.65 (m, 2H). ^{13}C NMR (125 MHz, DMSO-d_6): δ ppm 13.9, 14.2, 20.8, 22.1, 23.7, 28.7, 28.9, 29.2, 29.5, 31.3, 41.4, 53.5, 118.0, 126.3, 127.0, 128.8, 129.0, 133.6, 136.0, 136.8, 145.7, 151.0. Anal. calculated for $C_{47}H_{54}N_4$: C, 83.64; H, 8.06; N, 8.30. Found: C, 83.92; H, 8.02; N, 8.04.

*2.2.1.7. 10,10-Dioctyl-2,7-di-p-tolyl-6,10-dihydro-3H-fluoreno[2,3-d:6,7-d′]diimidazole (**3g**).* White solid, yield 75%. Mp 154–156 °C ^{1}H NMR (500 MHz, DMSO-d_6): δ ppm 0.52 (m, 4H), 0.68 (t, J = 7.1 Hz, 6H), 0.93–1.03 (m, 20H), 1.99 (m, 4H), 2.37 (s, 6H), 7.20–7.25 (m, 1H), 7.35 (d, J = 7.9 Hz, 4H), 7.42 (s, 1H), 7.59 (s, 1H), 7.86 (s, 1H), 8.09 (d, J = 7.7 Hz, 4H), 12.75–12.83 (m, 1H). ^{13}C NMR (125 MHz, DMSO-d_6): δ ppm 13.9, 21.1, 22.1, 23.7, 28.7, 28.9, 29.5, 31.2, 41.4, 53.5, 101.3, 105.1, 109.0, 112.6, 126.3, 126.7, 127.9, 128.9, 129.6, 134.8, 136.3, 137.0, 139.3, 142.7, 144.0, 144.7, 145.3, 151.4. Anal. calculated for $C_{45}H_{54}N_4$: C, 83.03; H, 8.36; N, 8.61. Found: C, 83.18; H, 8.52; N, 8.31.

*2.2.1.8. 2,7-Bis(4-methoxyphenyl)-10,10-dioctyl-6,10-dihydro-3H-fluoreno[2,3-d:6,7-d′]diimidazole (**3h**).* White powder, yield 40%. Mp 160–162 °C ^{1}H NMR (500 MHz, DMSO-d_6): δ ppm 0.51(m, 4H), 0.67 (m, 6H), 0.92–1.03 (m, 20H), 1.97 (m, 4H), 3.82 (s, 6H), 7.11 (m, 4H), 7.50 (m, 2H), 7.90 (m, 2H), 8.14 (m, 4H), 12.74 (m, 2H). ^{13}C NMR (125 MHz, DMSO-d_6): δ ppm 13.9, 22.1, 23.7, 28.7, 28.9, 29.6, 31.3, 41.4, 53.5, 55.4, 101.2, 108.2, 112.3, 114.5, 123.1, 127.9, 134.9, 136.5, 145.2, 151.4, 160.5. Anal. calculated for $C_{45}H_{54}N_4O_2$: C, 79.14; H, 7.97; N, 8.20; O, 4.69. Found: C, 79.35; H, 8.45; N, 8.02.

*2.2.1.9. 2,7-Bis(4-nitrophenyl)-10,10-dioctyl-6,10-dihydro-3H-fluoreno[2,3-d:6,7-d′]diimidazole (**3i**).* Yellow powder, yield 65%. Mp 187–188 °C ^{1}H NMR (500 MHz, DMSO-d$_6$): δ ppm0.47 (m, 4H), 0.63 (t, $J = 6.9$ Hz, 6H), 0.82–0.99 (m, 20H), 1.96 (m, 4H), 7.51 (s, 1H), 7.67 (s, 1H), 7.98 (m, 1H), 8.20–8.24 (m, 1H), 8.39–8.40 (m, 4H), 8.43–8.45 (m, 4H), 13.24–13.32 (m, 2H). ^{13}C NMR (125 MHz, DMSO-d$_6$): δ ppm 13.9, 22.0, 23.7, 28.7, 28.9, 29.5, 31.2, 41.3, 53.7, 102.0, 102.3, 105.6, 110.1, 113.4, 124.1, 124.4, 127.2, 135.3, 135.7, 136.4, 137.8, 138.0, 144.1, 144.5, 145.6, 146.1, 147.6, 149.1. Anal. calculated for $C_{43}H_{48}N_6O_4$: C, 72.45; H, 6.79; N, 11.79. Found: C, 72.48; H, 6.62; N, 11.90.

*2.2.1.10. 10,10-Dioctyl-2,7-bis(4-(trifluoromethyl)phenyl)-6,10-dihydro-3H-fluoreno[2,3-d:6,7-d′]diimidazole (**3j**).* Light yellow powder, yield 20%. Mp 181–182 °C ^{1}H NMR (500 MHz, DMSO-d$_6$): δ ppm 0.49 (m, 4H), 0.65 (t, $J = 7.1$ Hz, 6H), 0.89–0.97 (m, 20H), 1.98 (m, 4H), 7.49 (s, 1H), 7.66 (s, 1H), 7.90–7.91 (m, 4H), 7.95–7.97 (m, 1H), 8.18–8.22 (m, 1H), 8.40–8.42 (m, 4H), 13.10–13.19 (m, 2H). ^{13}C NMR (125 MHz, DMSO-d$_6$): δ ppm 13.9, 22.0, 23.7, 28.7, 28.8, 29.5, 31.2, 41.4, 53.6, 101.8, 102.1, 105.5, 109.6, 109.8, 113.1, 121.0123.2, 125.4, 126.0, 126.9, 127.5, 129.3, 129.6, 134.3, 135.1, 135.4, 136.5, 136.7, 137.4, 137.6, 143.9, 144.2, 145.2, 145.8, 146.7, 147.2, 149.7. Anal. calculated for $C_{45}H_{48}F_6N_4$: C, 71.22; H, 6.38; N, 7.38. Found: C, 71.35; H, 6.54; N, 7.21.

*2.2.1.11. 2,7-Bis(2-fluorophenyl)-10,10-dioctyl-6,10-dihydro-3H-fluoreno[2,3-d:6,7-d′]diimidazole (**3k**).* White powder, yield 51%. Mp 130–131 °C ^{1}H NMR (500 MHz, DMSO-d$_6$): δ ppm 0.50 (m, 4H), 0.64 (t, $J = 7.2$ Hz, 6H), 0.89–0.93 (m, 20H), 1.96–1.97 (m, 4H), 7.37 (m, 2H), 7.40 (d, $J = 8.8$ Hz, 1H), 7.42 (d, $J = 8.8$ Hz, 1H), 7.50–7.52 (m, 3H), 7.65 (s, 1H), 7.91–7.95 (m, 1H), 8.12–8.17 (m, 1H), 8.28 (m, 2H), 12.53–12.61 (m, 2H). ^{13}C NMR (125 MHz, DMSO-d$_6$): δ ppm 13.8, 22.0, 23.7, 28.7, 28.9, 29.5, 31.2, 41.5, 53.5, 102.0, 105.7, 109.2, 112.8, 116.4, 116.6, 118.5, 125.1, 126.1, 130.1, 131.5, 135.0, 136.5, 137.1, 143.4, 145.6, 146.4, 158.5, 160.5. Anal. calculated for $C_{43}H_{48}F_2N_4$: C, 78.39; H, 7.34; N, 8.50. Found: C, 78.65; H, 7.23; N, 8.38.

*2.2.1.12. 2,7-Bis(3-fluorophenyl)-10,10-dioctyl-6,10-dihydro-3H-fluoreno[2,3-d:6,7-d′]diimidazole (**3l**).* White powder, yield 48%. Mp 148–149 °C ^{1}H NMR (500 MHz, DMSO-d$_6$): δ ppm 0.50 (m, 4H), 0.65–0.70 (m, 6H), 0.91–1.01 (m, 20H), 1.97–1.99 (m, 4H), 7.29–7.32 (m, 2H), 7.47 (s, 1H), 7.57–7.61 (m, 3H), 7.64 (s, 1H), 7.95–8.00 (m, 2H), 8.04–8.06 (m, 2H), 8.14–8.19 (m, 1H), 12.94–13.03 (m, 2H). ^{13}C NMR (125 MHz, DMSO-d$_6$): δ ppm 13.9, 22.0, 23.7, 28.7, 28.8, 29.5, 31.2, 41.3, 53.6, 101.9, 105.3, 109.6, 113.0, 113.3, 114.2, 116.0, 116.4, 122.4, 125.2, 130.7, 131.1, 132.8, 134.9, 136.4, 137.2, 139.9, 142.5, 143.7, 145.1, 145.6, 147.0, 150.0, 151.7, 161.6, 163.5. Anal. calculated for $C_{43}H_{48}F_2N_4$: C, 78.39; H, 7.34; N, 8.50. Found: C, 78.49; H, 7.39; N, 8.27.

*2.2.1.13. 2,7-Bis(4-fluorophenyl)-10,10-dioctyl-3,6-dihydrofluoreno[2,3-d:6,7-d′]diimidazole (**3m**).* White powder, yield 54%. Mp 178–179 °C ^{1}H NMR (500 MHz, DMSO-d$_6$): δ ppm 0.52 (m, 4H), 0.69 (t, $J = 7.1$ Hz, 6H), 0.93–1.01 (m, 20H), 2.01–2.02 (m, 4H), 7.39–7.44 (m, 5H), 7.61 (s, 1H), 7.90 (m, 1H), 8.10–8.14 (m, 1H), 8.23–8.24 (m, 4H), 12.83–12.93 (m, 2H). ^{13}C NMR (125 MHz, DMSO-d$_6$): δ ppm 13.9, 22.0, 23.7, 28.7, 28.8, 29.5, 31.2, 41.3, 53.5, 101.7, 105.2, 109.1, 112.7, 116.0, 116.2, 127.2, 128.6, 134.9, 136.2, 136.9, 143.8, 144.1, 144.8, 145.4, 145.9, 146.4, 150.4, 162.0, 164.0. Anal. calculated for $C_{43}H_{48}F_2N_4$: C, 78.39; H, 7.34; N, 8.50. Found: C, 78.16; H, 7.21; N, 8.32.

*2.2.1.14. 2,7-Bis(2,6-difluorophenyl)-10,10-dioctyl-6,10-dihydro-3H-fluoreno[2,3-d:6,7-d′]diimidazole (**3n**).* Light yellow powder, yield 36%. Mp 169–170 °C ^{1}H NMR (500 MHz, DMSO-d$_6$): δ ppm 0.52 (s, 4H), 0.69 (t, $J = 7.1$ Hz, 6H), 0.94–1.04 (m, 20H), 2.02–2.03 (m, 4H), 7.32–7.35 (m, 4H), 7.49–7.50 (m, 1H), 7.60–7.66 (m, 2H), 7.69 (m, 1H), 7.97 (s, 1H), 8.19 (s, 1H), 12.81–12.90 (m, 2H). ^{13}C NMR (125 MHz, DMSO-d$_6$): δ ppm 13.9, 22.0, 23.7, 28.7, 28.8, 29.6, 31.2, 41.4, 53.6, 101.8, 102.0, 105.4, 105.5, 109.3, 109.4, 109.5, 109.7, 112.4, 112.6, 113.1, 132.3, 134.2, 134.4, 134.6, 136.2, 136.4, 137.2, 137.4, 140.9, 141.1, 143.4, 143.6, 143.8, 144.9, 145.4, 146.3, 146.9, 159.2, 159.3, 161.2, 161.3. Anal. calculated for $C_{43}H_{46}F_4N_4$: C, 74.33; H, 6.67; N, 8.06 Found: C, 74.53; H, 6.58; N, 8.12.

*2.2.1.15. 2,7-Bis(4-chlorophenyl)-10,10-dioctyl-6,10-dihydro-3H-fluoreno[2,3-d:6,7-d′]diimidazole (**3o**).* White powder, yield 46%. Mp 170–171 °C ^{1}H NMR (500 MHz, DMSO-d$_6$): δ ppm 0.48 (m, 4H), 0.65 (m, 6H), 0.89–1.01 (m, 20H), 1.97 (m, 4H), 7.45 (s, 1H), 7.61 (m, 5H), 7.91 (s, 1H), 8.12–8.15 (m, 1H), 8.21 (m, 4H), 12.92–13.00 (m, 2H). ^{13}C NMR (125 MHz, DMSO-d$_6$): δ ppm 13.9, 22.1, 23.7, 28.7, 28.9, 29.5, 31.2, 41.4, 53.5, 101.5, 101.8, 105.3, 109.5, 112.8, 128.0, 129.1, 129.4, 134.3, 134.9, 135.2, 136.3, 137.1, 137.3, 143.8, 144.1, 145.0, 145.5, 146.7, 150.2. Anal. calculated for $C_{43}H_{48}Cl_2N_4$: C, 74.66; H, 6.99; N, 8.10. Found: C, 74.18; H, 7.11; N, 8.05.

2.2.2. Synthesis of 4a and 4b

To a suspension of 3,6-dinitro-9,9-dioctylfluorene-2,7-diamine **1** (575 mg, 1.12 mmol) in ethanol (80 mL) was added Sn powder (802 mg, 6.8 mmol). The reaction mixture was heated to 90 °C with stirring, and concentrated hydrochloric acid (3 mL) was added to the solution by portions. And the solution was continued to be heated under reflux for about 30 min until **1** disappeared. The mixture was filtered and extracted with AcOEt for three times. The combined organic layer was washed with brine, dried over Na_2SO_4, filtered, and then the solvent was evaporated in vacuum. The obtained yellow residue 2,3,6,7-tetraamino-9,9-dioctylfluorene **2b** was directly used for next step without further purification.

A mixture of the above obtained 9,9-dioctylfluorene-2,3,6,7-tetraamine (**2b**) and benzaldehyde (235 mg, 2.22 mmol) were heated to 100 °C in 1,4-dioxane for about 10 h. The solvent was removed under vacuum and the residue was purified by flash column chromatography using petroleum ether/ethyl acetate as eluent to afford the desired compounds.

*2.2.2.1. 3-Benzyl-10,10-dioctyl-2,7-diphenyl-6,10-dihydro-3H-fluoreno[2,3-d:6,7-d′]diimidazole (**4a**).* Light yellow powder, yield 19–23%. Mp 89–91 °C ^{1}H NMR (500 MHz, DMSO-d$_6$): δ ppm 0.64 (s, 4H), 0.79 (m, 6H), 0.99–1.06 (m, 20H), 1.96 (m, 4H), 5.48 (s, 1H), 5.52 (s, 1H), 7.08–7.12 (m, 1H), 7.21–7.23 (m, 2H), 7.29–7.32 (m, 2H), 7.34 (m, 1H), 7.35–7.36 (m, 1H), 7.38–7.42 (m, 6H), 7.50 (s, 1H), 7.67–7.71 (m, 4H), 8.18 (d, $J = 7.2$ Hz, 1H), 12.15 (s, 1H). ^{13}C NMR (125 MHz, CDCl$_3$): δ ppm 13.8, 22.3, 23.7, 29.1, 29.4, 29.8, 30.0, 31.2, 31.5, 41.6, 48.3, 53.7, 53.9, 100.7, 104.9, 109.5, 113.2, 113.3, 125.7, 125.9, 127.1, 127.6, 127.9, 128.5, 128.6, 128.7, 128.9, 129.0, 129.3, 129.4, 129.7, 129.8, 132.0, 135.6, 135.7, 136.1, 136.2, 136.5, 137.0, 137.4, 137.7, 141.8, 142.2, 142.3, 146.4, 146.8, 147.6, 152.2, 153.7, 169.7. ESI-MS (*m*/*z*): 713.4 $[M + H]^+$. Anal. calculated for $C_{50}H_{56}N_4$: C, 84.23; H, 7.92; N, 7.86. Found: C, 84.07; H, 8.01; N, 7.73.

*2.2.2.2. 3,6-Dibenzyl-10,10-dioctyl-2,7-diphenyl-6,10-dihydro-3H-fluoreno[2,3-d:6,7-d′]diimidazole (**4b**).* Light yellow powder, yield 16–24%. Mp 174–176 °C ^{1}H NMR (500 MHz, CDCl$_3$): δ ppm 0.73 (m, 4H), 0.80 (t, $J = 7.2$ Hz, 6H), 1.05–1.12 (m, 20H), 2.07–2.11 (m, 4H), 5.48 (s, 4H), 7.17–7.19 (d, $J = 7.4$ Hz, 4H), 7.32 (m, 2H), 7.37 (m, 4H), 7.42–7.46 (m, 8H), 7.68 (d, $J = 6.9$ Hz, 4H), 7.78 (s, 2H). ^{13}C NMR (125 MHz, DMSO-d$_6$): δ ppm 13.9, 22.4, 23.8, 29.2, 29.5, 30.0, 31.6, 41.7, 48.3, 53.9, 100.4, 113.7, 125.8, 127.6, 128.0, 128.6, 129.0, 129.5, 129.7, 129.8, 132.5, 135.8, 136.4, 137.3, 142.7, 147.2, 153.9. ESI-MS

(m/z): 804.5 $[M + H]^+$. Anal. calculated for $C_{57}H_{62}N_4$: C, 85.24; H, 7.78; N, 6.98. Found: C, 85.10; H, 7.55; N, 6.87.

2.3. *Determination of crystal structure of 4b*

Suitable single crystals of **4b** for X-ray structural analysis were obtained by slow evaporation of a solution of the solid in dichloromethane and methanol at room temperature. The selected crystal with approximate dimensions of 0.25 × 0.20 × 0.20 mm for **4b** was mounted on a four-circle single crystal X-ray diffractometer (CAD4 DIFFACTIS 586) using a graphite monochromated MoKα radiation ($\lambda = 0.071073$ nm) and the data were collected at 296(2) K. The structure was solved by direct methods and refined by full-matrix least-squares method on F^2_{obs} by using the SHELXTL 97 software package. The non-hydrogen atoms were refined anisotropically. The hydrogen atoms bound to carbon were located by geometrical calculations, with their position and thermal parameters being fixed during the structure refinement. The final refinement converged at $R_1 = 0.1352$, $wR_2 = 0.3435$ for **4b**. A summary of the crystallographic data and structure refinement details is given in Table 1. The crystal structure and cell structure of **4b** are shown in Fig. 3.

3. Result and discussion

3.1. *Synthesis*

The synthetic strategy employed involved the efficient preparation of the key intermediate 2,3,6,7-tetraamino-9,9-dioctylfluorene (TADOF, **2a**) from fluorene. A systematic synthetic route for 2,3,6,7-tetraamino-9,9-bisalkylfluorene was reported by Qian's group [40]. In our synthesis, we modified the final step and 3,6-dinitro-9,9-dioctylfluorene-2,7-diamine (**1**) was hydrogenised with $Pd(OH)_2$ and hydrazine hydrate in EtOH under reflux to yield TADOF (**2a**), which was used for next step without further purification after the work-up. By condensation of **2a** with the corresponding aldehydes in 1.4-dioxane at 100 °C for about 10 h, fifteen aromatic substituted 6,10-dihydrofluoreno[2,3-*d*:6,7-*d*′]diimidazole derivatives **3a-o** were successfully obtained in total 20–75% yields by two steps (Fig. 1). During exploration of the final hydrogenated step, when tin powder was used as the reducing agent, an alternate intermediate **2b** was obtained. By condensation of **2b** with benzaldehyde, a mixture of two alkylated compounds **4a** and **4b**, as well as **3a** was obtained. This may be caused by the existed Sn^{4+} having not been completely removed after the work-up procedure (Fig. 2). This assumption was confirmed by adding Sn^{4+} into the condensation reaction of **2a** with benzaldehyde and three compounds were obtained with the ratio slightly different. All target compounds were isolated and purified by column chromatography on silica gel with high purity and their molecular structures were confirmed by ^1H NMR spectroscopy, ^{13}C NMR spectroscopy, and element analysis, which were shown detailed in experiment section.

Table 1
Crystal data and structure refinement for **4b.**

Empirical formula	$C_{57}H_{62}N_4$
Formula weight	803.11
Temperature (K)	296(2) K
Wavelength (Å)	0.71073 Å
Crystal system, space group	Triclinic, P-1
Unit cell dimensions	
a (Å)	13.500(3)
b (Å)	14.957(3)
c (Å)	15.611(3)
α (°)	66.689(3)
β (°)	71.951(3)
γ (°)	82.431(3)
Volume (Å^3)	2752.3(10)
Z	2
Density (calc.) (Mg/m^3)	0.969
Absorption coefficient (mm^{-1})	0.056
F(000)	864
Crystal size (mm)	0.25 × 0.20 × 0.20 mm
θ range for data collection (°)	1.97–25.05
Limiting indices	$-16 \le h \le 8, -17 \le k \le 16, -18 \le l \le 18$
Reflections collected/unique	14342/9557 [*R*(int) = 0.0227]
Completeness to theta = 25.05	98.0%
Absorption correction	None
Max. and min. transmission	0.9889 and 0.9861
Refinement method	Full-matrix least-squares on F^2
Data/restraints/parameters	9557/2/517
Goodness-of-fit on F^2	1.213
Final *R* indices [I > 2σ(I)]	$R_1 = 0.1352$, $wR_2 = 0.3435$
R indices (all data)	$R_1 = 0.2054$, $wR_2 = 0.4030$
Largest diff. Peak and hole (eÅ^{-3})	1.038 and −0.324
CCDC deposit no.	CCDC 873787

3.2. *X-ray crystallography analysis*

The spatial structure of compound **4b** was determined by using X-ray diffraction analysis. The ORTEP view of the structure of **4b** (Fig. 3a) showed the almost planar arrangement of the 6,10-dihydrofluoreno[2,3-*d*:6,7-*d*′]diimidazole ring. The fluorene moiety ii forms dihedral angle of 0.31° with adjacent imidazole ring iii. In contrast, the adjacent phenyl ring iv takes a torsion angle of 41.24° with the 6,10-dihydrofluoreno[2,3-*d*:6,7-*d*′]diimidazole moiety. In the crystal lattice (Fig. 3b), the molecules are stacked in a head-to-tail manner and the alignment is mainly caused by weak intermolecular Van der Waals force.

3.3. *Spectral properties*

The photophysical properties of the compounds were examined by UV–vis and photoluminescent (PL) spectra in dilute CH_2Cl_2 and in the solid films, as shown in Figs. 4 and 5. The absorption peak wavelengths (λ_{abs}), fluorescence excitation wavelengths (λ_{ex}), PL peak wavelengths (λ_{em}), stokes shift ($\lambda_{em}-\lambda_{ex}$) in solution and the solid state, and fluorescence quantum yields (φ_{FL}) in solution are collected in Table 2. The UV–vis and PL spectra in the solid state were carried out on films spin-coated onto quartz from chloroform solution. The results showed that the absorption maxima of these 6,10-dihydrofluoreno[2,3-*d*:6,7-*d*′]diimidazole derivatives in CH_2Cl_2 solution vary from 363 to 423 nm that are attributed to the $\pi-\pi^*$ transition depending on the substituents at the terminal position. As it can be observed in Fig. 4a, compound **3a** bearing phenyl group at the terminal exhibited the absorption maximum at 366 nm in CH_2Cl_2. With the change of the substituents at the terminal position from the phenyl to other aryl group such as thiophen-2-yl (**3b**), 5-methylfuran-2-yl (**3c**), pyridin-2-yl (**3d**), naphthalen-1-yl (**3e**) and (*E*)-styryl (**3f**), the UV–vis absorption maxima were all red-shifted. Compounds **3b** and **3e** exhibited strong $\pi-\pi^*$ electron absorption bands, which peak at 382 and 372 nm, respectively. The absorption spectra of compounds **3c** and **3d** were very similar, showing two characteristic absorption peaks at ca. 376 and 388 nm. And the largest red-shift was observed at 396 nm for compound **3f**, which possesses the longest conjugation length, relative to that of the other compounds. Moreover, it can be found that compounds **4a-b** with benzyl in N-1 positions have almost the same absorption maxima as compound **3a**, indicating that alkylation of imidazole has a limited effect on their electric energy levels.

Next, in order to study the substituent effect on the optical properties, a series of compounds (**3g-o**) with various polar groups

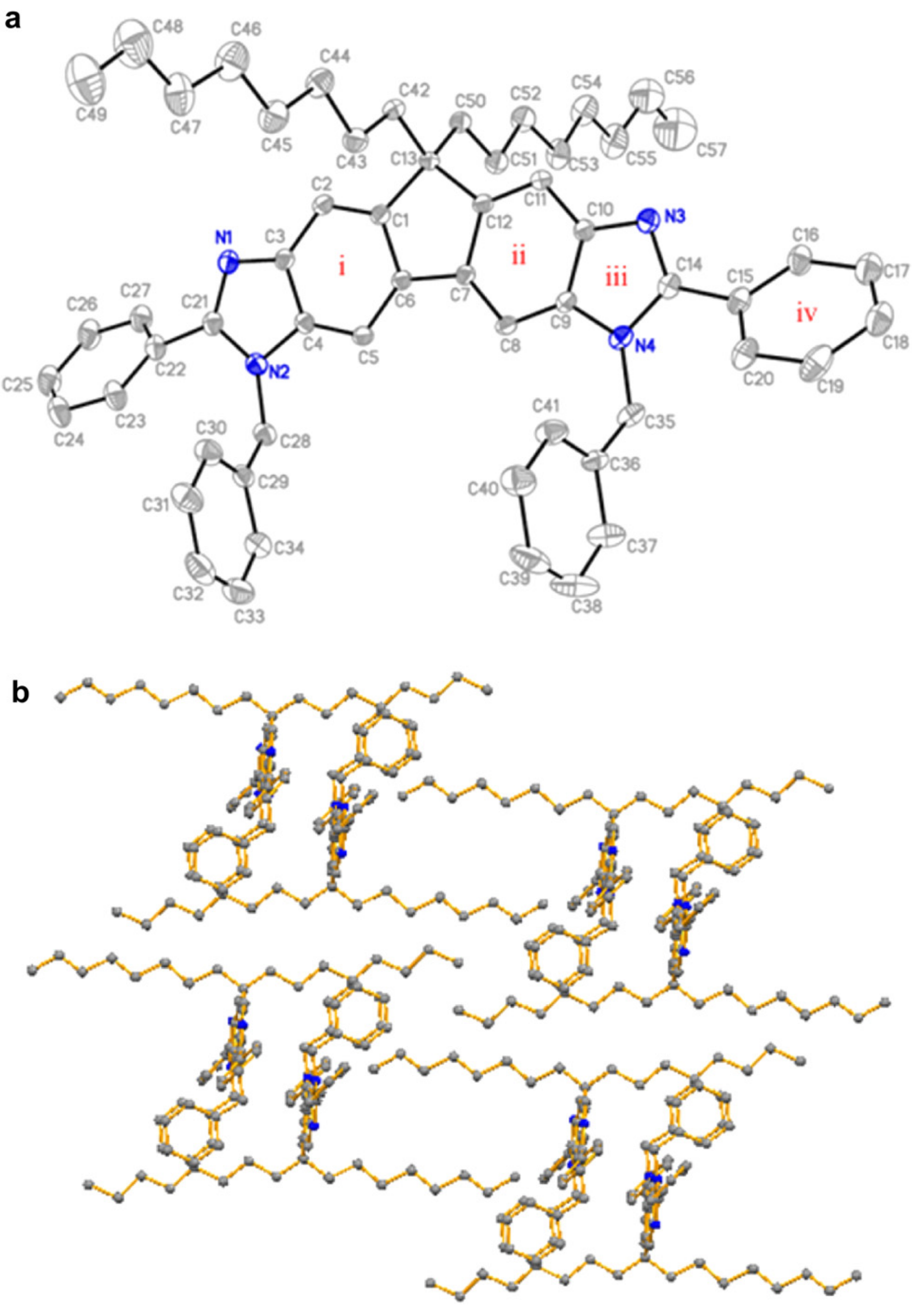

Fig. 3. The molecular structures of compound **4b**, H atoms and the molecular structures of solvents are omitted for clarity. (a) ORTEP drawing. (b) A view of the molecule packing structure.

(F, Cl, CH_3, CF_3, NO_2, OMe) substituted on the phenyl ring were studied. Among these polar groups, some are known as strong π-acceptors (i.e., NO_2), others are known as intermediate (i.e. F, Cl), besides being classified as electron-withdrawing (i.e., F, Cl, CF_3, NO_2) or electron-donating groups (i.e., CH_3, OMe). Compared with the maximum absorption peak of compound **3a** (366 nm), compounds **3g** (371 nm) and **3h** (373 nm) with electron-donating methyl and methoxyl groups, respectively, had slight shifts toward higher wavelengths. Compound **3j** with electron-withdrawing CF_3 group exhibited the absorption maximum at 378 nm. Moreover, compound **3k** with fluorine group in *ortho*-position of the terminal benzene ring showed two absorption peaks, one at 370 nm and the other at 385 nm. The UV–vis absorption maxima of **3l**, **3m, 3n** and **3o** were red-shifted by 4, 0, 2, 7 nm respectively relative to that of **3a**, and the enormous red-shift of 57 nm as observed in **3i** with a broad and featureless absorption band. The effect of the substituent on the absorption properties is not clearly seen. This suggests that the electronic properties of the substituents might not play an important role in the UV–vis absorption spectra.

According to the electronic absorption spectra of **3a-f**, **4a-b** in thin films, as shown in Fig. 4b, all compounds showed red-shifted absorption maxima by 5–30 nm by comparison with the dilute CH_2Cl_2 solutions and the enormous red-shift of 30 nm as observed

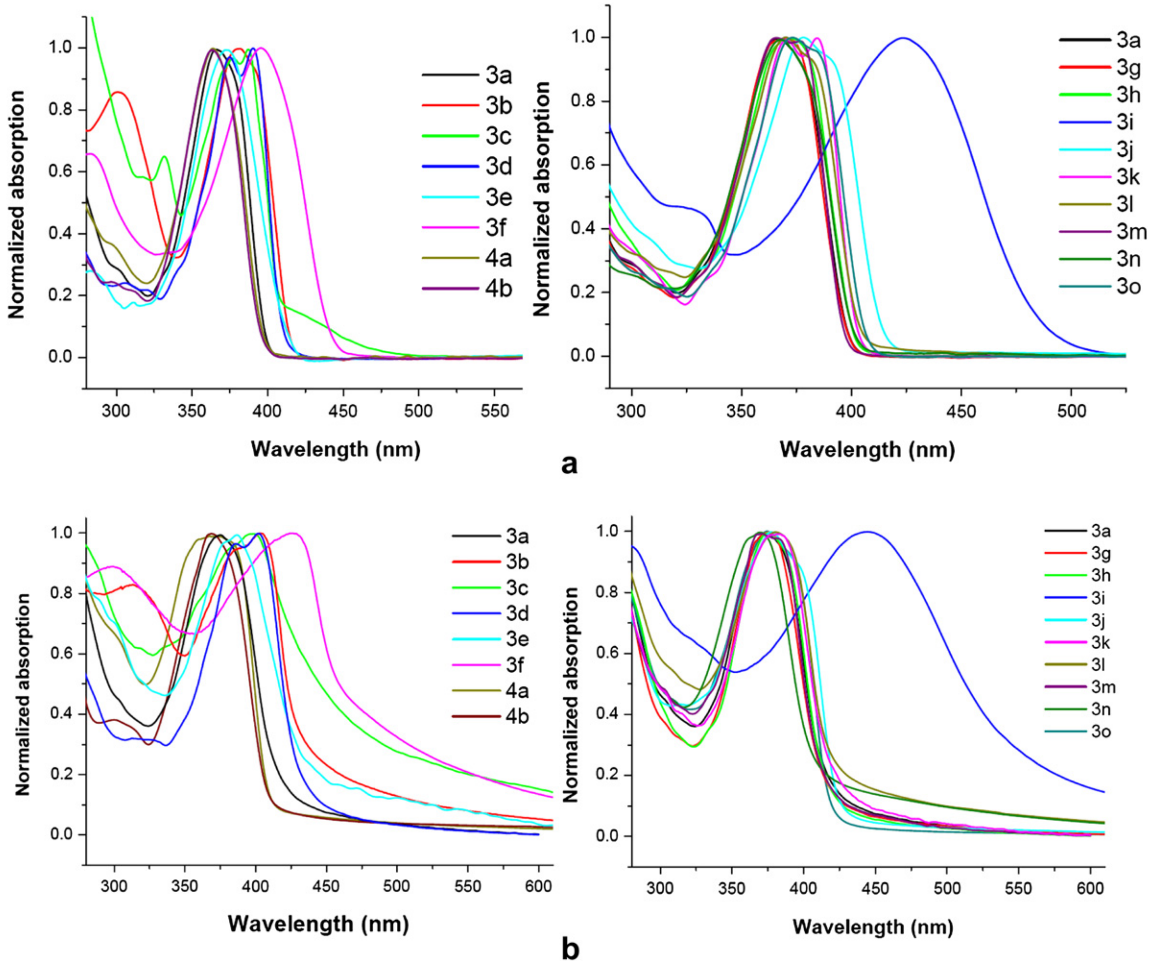

Fig. 4. Normalized absorption spectra of **3a-o**, **4a-b** (1×10^{-5} M) recorded in CH_2Cl_2 solutions (a) and thin neat films (b) at room temperature.

in **3f** with a broad and featureless absorption band at ca. 426 nm. Regarding the absorption spectra of **3g-o** in films, the trends observed with different substituents in terms of the spectral shapes and peak positions were nearly the same compared to the spectra obtained in dilute solutions. And the UV–vis absorption maxima of compounds **3a**, **3g-h**, **3j** and **3o** were almost the same at ca. 375 nm. The UV–vis absorption maxima of **3n**, **3m**, **3l** and **3i** were red-shifted by 2, 4, 10 and 20 nm respectively relative to those in dilute CH_2Cl_2 solution and compound **3k** showed a slightly blue shift.

Fig. 5 shows the photoluminescence (PL) spectra recorded upon excitation at each excitation wavelength (λ_{ex}) at room temperature. In CH_2Cl_2 solution, the fluorescence spectra of **3a** showed two peaks at 395 and 416 nm (Fig. 5a) and the fluorescence quantum yield is 0.78, which is higher than that of quinine sulfate ($\varphi_{FL} = 0.55$). The fluorescence spectra of compounds **3c** and **4b** were almost the same as those of **3a**, showing two peaks at 396 and 417 nm, whereas compound **4a** ($\lambda_{em} = 392$, 412 nm) showed slightly blue-shifted PL spectra by 3 nm. The fluorescence spectra of compound **3b** with two peaks at 409 and 426 nm were red-shifted by 10 nm relative to those of **3a**. It's interesting to note that the fluorescence maxima of **3d**, **3e** and **3f**, relative to those of **3a**, were red-shifted by 12, 26 and 38 nm, respectively, and compound **3f** fluoresced in dichloromethane with emission peaks at ca. 454 nm, probably due to the elongation of the conjugation length.

The PL spectra of compounds **3a**, **3g-h** and **3k-o** in CH_2Cl_2 were very similar in shape. The fluorescence spectra of compounds **3g-h, 3k-l,** and **3n** were very similar to those of **3a** with two peaks at ca. 395 and 416 nm. Compared to **3a**, compound **3o** ($\lambda_{em} = 401$, 420 nm) with *para*-Cl substituted phenyl group at the terminal red-shifted ca. 5 nm, whereas compound **3m** ($\lambda_{em} = 387$, 409 nm) with *para*-F blue-shifted by 7 nm. Compound **3j** fluoresced in dichloromethane with emission peaks at 431 nm, probably due to the increased charge-transfer character induced by the fluoroalkyl group. Compound **3i** exhibited quite weak fluorescence in solution and in thin films owing to the existence of nitro-substituent, which would decrease the radiative rate and increase the internal conversion rate of an excited state fluorophore [41]. Except compound **3i**, all the other compounds synthesized were moderate to high fluorescent in CH_2Cl_2 solution with fluorescence quantum yields φ_{FL} in the range of 0.30–0.89.

By comparison with the dilute CH_2Cl_2 solutions, the emission spectra of all compounds in solid states showed red-shifts to longer wavelengths by 20–74 nm (Fig. 5b). The red-shifts of the emission observed in the solid state were probably due to the rigid 6,10-dihydrofluoreno[2,3-*d*:6,7-*d*′]diimidazole group and its strong intermolecular forces, which drove the molecules to pack at high density, restricted the molecular rotation and increased the π-conjugation significantly, in turn resulting in the red-shifts. Concerning the larger stokes shift (λ_{em}–λ_{ex}) of compounds **3a-h**, **3j-o** and **4a-b** in the film state as compared with those in the solution phase, it can be explained in the same way. In the solid state, the fluorescence maxima of **3a** were red-shifted by ca. 39 nm relative to those in CH_2Cl_2 solution, showing one peak at 455 nm. Derivatives

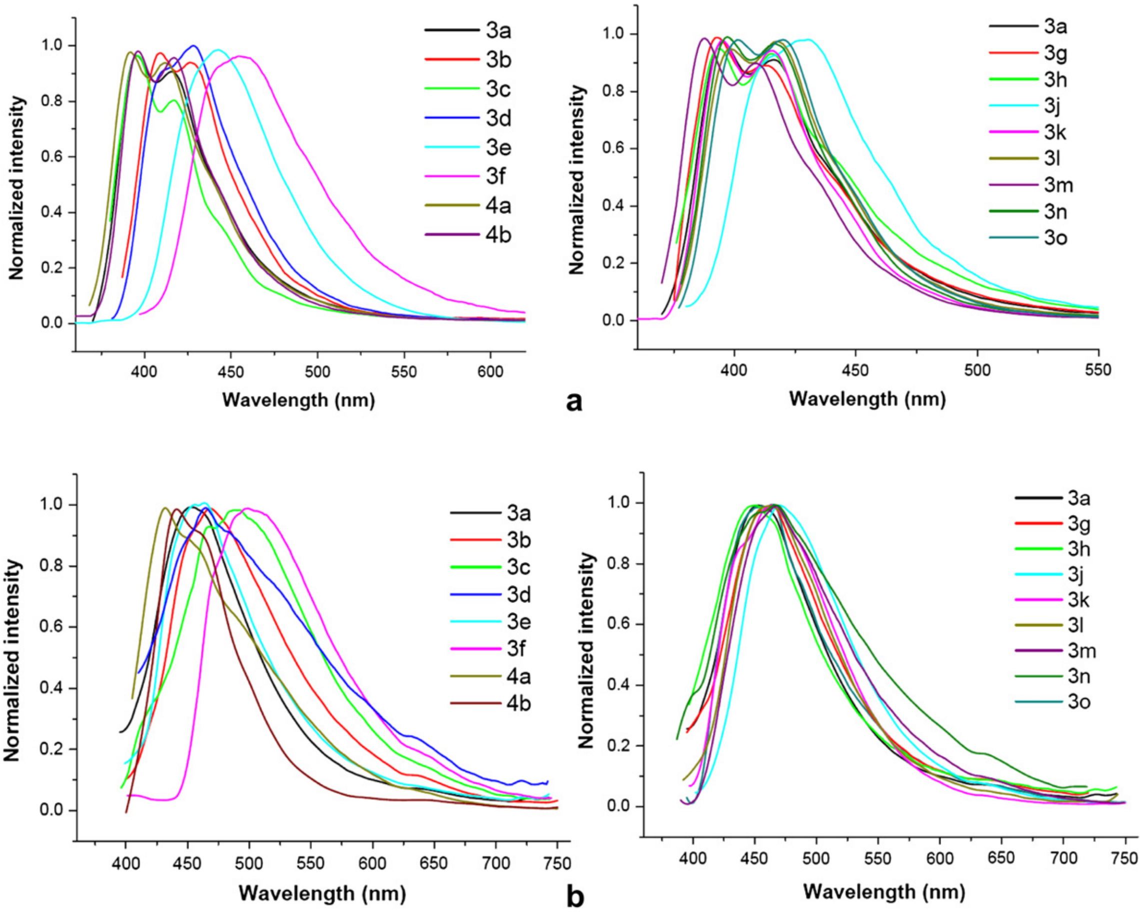

Fig. 5. Normalized fluorescence spectra of **3a-o**, **4a-b** (1×10^{-6} M) recorded in CH_2Cl_2 solutions (a) and thin neat films (b) excited at each λ_{ex} at room temperature.

3c and **3f** showed blue-green emission, with PL emission maxima at 491 and 498 nm, respectively. Besides compounds **3h**, **4a** and **4b** (λ_{max} = 450, 432 and 441 nm, respectively), all other compounds **3b**, **3d-e**, **3g** and **3j-o** showed blue PL with λ_{max} between 462 and 470 nm in their solid states.

It is worth mentioning that both the absorption and emission maxima of **3a**, **3g, 3j, and 3m-o** in solution and in the solid state are red-shifted from those of their fluoreno[2,3-*d*]imidazole counterparts (e.g., the λ_{abs} in CH_2Cl_2, λ_{em} in CH_2Cl_2 and in the solid state of compound **3a**, relative to those of compound DOFIPh [39], were

Table 2
Optical properties of the compounds **3a-o**, **4a-b**.

Compound	λ_{abs}(nm)[a]		λ_{ex}(nm)[b]		λ_{em}(nm)[c]		Stokes shifts (nm)[d]		φ_{FL}[e]
	CH_2Cl_2	film	CH_2Cl_2	film	CH_2Cl_2	film	CH_2Cl_2	film	
3a	366	375	366	375	395, 416	455	29	80	0.78
3b	382	403	383	405	409, 426	468	26	63	0.42
3c	377, 387	398	377	400	396, 417	491	19	91	0.64
3d	375, 390	386, 402	376	387	428	465	52	78	0.61
3e	372	387	374	387	442	464	68	77	0.61
3f	396	426	396	426	454	498	58	72	0.33
3g	371	376	372	376	393, 413	464	21	88	0.85
3h	373	375	371	378	393, 415	450	22	72	0.8
3i	423	443	–	–	–[f]	–[f]	–	–	0.01
3j	378	377	380	383	431	470	51	87	0.3
3k	370, 385	383	372	383	395, 416	464	23	81	0.81
3l	370	380	373	383	398, 417	462	25	79	0.79
3m	366	370	377	378	387, 409	468	10	90	0.82
3n	368	370	374	378	397, 416	467	23	89	0.63
3o	373	374	373	382	401, 420	464	28	82	0.89
4a	364	373	365	381	392, 412	432	27	51	0.72
4b	363	368	366	376	396, 417	441	30	65	0.67

[a] UV–vis absorption wavelengths in dichloromethane or in thin neat films at room temperature.
[b] Excitation wavelengths in dichloromethane or in thin neat films at room temperature.
[c] Fluorescence wavelengths in dichloromethane or in thin neat films at room temperature.
[d] Stokes shift (λ_{em}–λ_{ex}) in dichloromethane or in thin neat films at room temperature.
[e] Fluorescence quantum yields, measured in CH_2Cl_2 solution using a 0.2 M H_2SO_4 solution of quinine sulfate (φ_{FL} = 0.55) as a reference.
[f] Too weak to be measured.

red-shifted by 26, 31 and 13 nm, respectively), indicating fusion of another aryl-imidazole unit is effective for extending π conjugation.

4. Conclusion

In summary, 2,3,6,7-tetraamino-9,9-dioctylfluorene (TADOF), as a new multifunctional intermediate for π-conjugated molecules, was efficiently synthesized. And novel 10,10-dioctyl-3,6-dihydrofluoreno[2,3-*d*:6,7-*d*′]diimidazole (DOFDI)-type fluorophores with various aryl substituents were designed and conveniently synthesized, and their absorption and fluorescence properties were investigated in solution and in the solid state. The DOFDIs were synthesized by condensation of the key intermediate TADOF with aldehydes under very mild conditions, which make it possible to incorporate a diverse range of substituents in the DOFDI core and provided an efficient approach to the preparation of some useful dyes and pigments. It can be concluded that the absorption spectra and fluorescence characteristics of the new target compounds show dependence on their molecular structure. These compounds possess a medium strong blue fluorescence-emitting ability with φ_{FL} values in the region of 0.30–0.89. Further research regarding the incorporation of these systems usable both as organic light-emitting diodes and as fluorescent probes is under way in our laboratory.

Acknowledgements

The authors are grateful for support from the National Natural Science Foundation of China (Project No. 30672506), Shanghai Pujiang Program (No. 10PJ1403700), and Leading Academic Discipline Project of Shanghai Municipal Education Commission (Project No. J50102). H.-F.C. thanks the support of the 5th Innovation Foundation of Shanghai University.

References

[1] Tang CW, VanSlyke SA. Organic electroluminescent diodes. Appl Phys Lett 1987;51:913–5.

[2] Burroughes JH, Bradley DDC, Brown AR, Marks RN, Mackay K, Friend RH, et al. Light-emitting diodes based on conjugated polymers. Nature 1990;347:539–41.

[3] Baldo MA, Thompson ME, Forrest SR. High-efficiency fluorescent organic light-emitting devices using a phosphorescent sensitizer. Nature 2000;403:750–3.

[4] Welter S, Brunner K, Hofstraat JW, Cola LD. Electroluminescent device with reversible switching between red and green emission. Nature 2003;421:54–7.

[5] Brabec CJ, Sariciftci NS, Hummelen JC. Plastic solar cells. Adv Funct Mater 2001;11:15–26.

[6] McGehee MD, Heeger AJ. Semiconducting (conjugated) polymers as materials for solid-state lasers. Adv Mater 2000;12:1655–68.

[7] Schon JH, Dodabalapur A, Kloc C, Batlogg B. A light-emitting field-effect transistor. Science 2000;290:963–5.

[8] Beaupre S, Boudreault P-LT, Leclerc M. Solar-energy production and energy-efficient lighting: photovoltaic devices and white-light-emitting diodes using Poly(2,7-fluorene), Poly(2,7-carbazole), and Poly(2,7-dibenzosilole) derivatives. Adv Ener Mater 2010;22:E6–27.

[9] Xiao LX, Chen ZJ, Qu B, Luo JX, Kong S, Gong QH, et al. Recent progresses on materials for Electrophosphorescent organic light-emitting devices. Adv Mater 2011;23:926–52.

[10] Burn PL, Lo S-C, Samuel IDW. The development of light-emitting dendrimers for displays. Adv Mater 2007;19:1675–88.

[11] Chen SF, Deng LL, Xie J, Peng L, Xie LH, Fan QL, et al. Recent developments in top-emitting organic light-emitting diodes. Adv Mater 2010;22:5227–39.

[12] Rogach AL, Gaponik N, Lupton JM, Bertoni C, Gallardo DE, Dunn S, et al. Light-emitting diodes with semiconductor nanocrystals. Angew Chem Int Edit 2008;47:6538–49.

[13] Hwang SH, Moorefield CN, Newkome GR. Dendritic macromolecules for organic light-emitting diodes. Chem Soc Rev 2008;37:2543–57.

[14] Farinola GM, Ragni R. Electroluminescent materials for white organic light emitting diodes. Chem Soc Rev 2011;40:3467–82.

[15] Zhu XH, Peng JB, Cao Y, Roncali J. Solution-processable single-material molecular emitters for organic light-emitting devices. Chem Soc Rev 2011;40:3509–24.

[16] Yokoyama D. Molecular orientation in small-molecule organic light-emitting diodes. J Mater Chem 2011;21:19187–202.

[17] Lo SC, Burn PL. Development of dendrimers: macromolecules for use in organic light-emitting diodes and solar cells. Chem Rev 2007;107:1097–116.

[18] Lee TW, Lim KG, Kim DH. Approaches toward efficient and stable electron extraction contact in organic photovoltaic cells: inspiration from organic light-emitting diodes. Electron Mater Lett 2010;6(1):41–50.

[19] Fantacci S, Angelis FD. A computational approach to the electronic and optical properties of Ru (II) and Ir (III) polypyridyl complexes: applications to DSC, OLED and NLO. Coordin Chem Rev 2011;255:2704–26.

[20] Zhou GJ, Wong WE, Suo S. Recent progress and current challenges in phosphorescent white organic light-emitting diodes (WOLEDs). J Photoch Photobio C 2010;11:133–56.

[21] Danel A, Gondek E, Kityk I. 1*H*-pyrazolo[3,4-*b*]quinoline and 1*H*-pyrazolo[3,4-*b*]quinoxaline derivatives as promising materials for optoelectronic applications. Opt Mater 2009;32:267–73.

[22] Grimsdale AC, Chan KL, Martin RE, Jokisz PG, Holmes AB. Synthesis of light-emitting conjugated polymers for applications in electroluminescent devices. Chem Rev 2009;109:897–1091.

[23] Beaujuge PM, Frechet JMJ. Molecular design and ordering effects in π-functional materials for transistor and solar cell applications. J Am Chem Soc 2011;133:20009–29.

[24] Grell M, Bradley DDC, Ungar G, Hill J, Whitehead KS. Interplay of physical structure and photophysics for a liquid crystalline polyfluorene. Macromolecules 1999;32:5810–7.

[25] Jenekhe SA, Osaheni JA. Excimers and exciplexes of conjugated polymers. Science 1994;265:765–8.

[26] Han J, An J, Im C, Cho NS, Shim HK, Majima T. Comparing electroluminescence efficiency and photoluminescence quantum yield of fluorene-based π-conjugated copolymers with narrow band-gap comonomers. J Photoch Photobio A 2009;205:98–103.

[27] Setayesh S, Grimsdale AC, Weil T, Enkelmann V, Müllen K, Meghdadi F, et al. Polyfluorenes with polyphenylene dendron side chains: toward non-aggregating, light-emitting polymers. J Am Chem Soc 2001;123:946–53.

[28] Marsitzky D, Scott JC, Chen J-P, Lee VY, Miller RD, Setayesh S, et al. Poly-2,8-(indenofluorene-*co*-anthracene)–a colorfast blue-light-emitting random copolymer. Adv Mater 2001;13:1096–9.

[29] Li ZH, Wong MS, Fukutani H, Tao Y. Full emission color tuning in bis-dipolar diphenylamino-endcapped oligoarylfluorenes. Chem Mater 2005;17:5032–40.

[30] Yasuda T, Fujita K, Tsutsui T. Carrier transport properties of monodisperse Glassy-Nematic oligofluorenes in organic field-effect transistors. Chem Mater 2005;17:264–8.

[31] Lai W-Y, Zhu R, Fan Q-L, Hou L-T, Cao Y, Huang W. Monodisperse six-armed triazatruxenes: microwave-enhanced synthesis and highly efficient pure-deep-blue electroluminescence. Macromolecules 2006;39(11):3707–9.

[32] Leclerc M. Polyfluorenes: twenty years of progress. J Polym Sci Pol Chem 2001;39:2867–73.

[33] Neher D. Polyfluorene homopolymers: conjugated liquid-crystalline polymers for bright blue emission and polarized electroluminescence. Macromol Rapid Comm 2001;22:1365–85.

[34] Scherf U, List EJM. Semiconducting polfluoenes - towards reliable structure-property Relationships. Adv Mater 2002;14:477–87.

[35] Wong K-T, Hwu T-Y, Balaiah A, Chao T-C, Fang F-C, Lee C-T, et al. Modulation of physical properties of Ter(9,9-ditolylfluorene) by backbone-embedded heteroarenes. Org Lett 2006;8(7):1415–8.

[36] Tao YX, Xu QF, Lu JM, Yang XB. The synthesis, electrochemical and fluorescent properties of monomers and polymers containing 2,5-diphenyl-1,3,4-thiadiazole. Dyes Pigm 2010;84:153–8.

[37] Yan YN, Pan WL, Song HC. The synthesis and optical properties of novel 1,3,4-oxadiazole derivatives containing an imidazole unit. Dyes Pigm 2010;86:249–58.

[38] Li XW, He DH. Synthesis and optical properties of novel anthracene-based stilbene derivatives containing an 1,3,4-oxadiazole unit. Dyes Pigm 2012;93:1422–7.

[39] Guo JG, Cui YM, Lin HX, Xie XZ, Chen HF. New fluorene derivatives based on 3,9-dihydrofluoreno[3,2-*d*]imidazole (FI): characterization and influence of substituents on photoluminescence. J Photoch Photobio A 2011;219:42–9.

[40] Li XC, Xiao Y, Qian XH. 2,3,6,7-Tetraamino-9,9-bis(2-ethylhexyl)fluorene: new multifunctional monomer for soluble ladder-conjugated molecules and Polymers. Org Lett 2008;10(13):2885–8.

[41] Kotaka H, Konishi G-I, Mizuno K. Synthesis and photoluminescence properties of π-extended fluorene derivatives: the first example of a fluorescent solvatochromic nitro-group-containing dye with a high fluorescence quantum yield. Tetrahedron Lett 2010;51:181–4.